Extended Frequency Divider Formula with Inclusion of DER Control Dynamics

Mohammadamin Aghahassani
Edgardo D. Castronuovo, *Senior IEEE*, Pablo Ledesma
Universidad Carlos III de Madrid
Madrid, Spain
maghahas@ing.uc3m.es

Federico Milano, *IEEE Fellow*
School of Electrical & Electronic Engineering
University College Dublin
Dublin, Ireland
federico.milano@ucd.ie

***Abstract*—This paper extends the recently proposed frequency divider formula (FDF) to account for the effect of the frequency control capability of distributed energy resources (DERs) on local voltage frequency variations. Both grid-forming and grid-following controllers are considered and formulated in order to resemble the same structure of synchronous machines. The proposed extension is applied to a modified dynamic model of the IEEE 118-bus test system and compared with the original FDF.**

***Index Terms*—Distributed energy resources, frequency divider, frequency estimation, grid-following, grid-forming.**

I. Introduction

A. Motivation

Evaluating the impact of each device on local as well as system-wide frequency variations has become a relevant concern for system operators [1]. In this vein, the frequency divider formula (FDF) proposed in [2] is a mathematical-based technique that approximately yet effectively estimates system bus frequencies. This formula is based on a boundary value problem where synchronous machines (SMs) rotor speeds set boundary conditions. It means that, based on the FDF, the frequencies of all system buses, including SMs, DERs, and load buses, can be linearly expressed by SMs rotor speeds. However, [2] assumes that SMs are the only devices that can modify the frequency at their connection buses to the grid. An extension of the FDF is proposed in [3], which allows taking into account any regulating device, assuming that one can properly define the quota of the rate of change of active powers (RoCoPs) at network buses that impact exclusively on the frequency. Thus, the formulation in [3] leaves open the question of which is a convenient expression of the RoCoPs of DERs, and, more specifically, of their controllers. This paper addresses this question precisely and proposes a generalization of the FDF able to include, using approximations similar to those utilized for the original FDF, both grid-forming and grid-following control strategies of DERs.

M. Aghahassani is supported by Spanish Agencia Estatal de Investigación, under the project AEI/10.13039/501100011033 (grant no. PID2019-104449RB-I00).

F. Milano is supported by Sustainable Energy Authority of Ireland (SEAI), under the project FRESLIPS (grant no. RDD/00681) and by the European Commission, under the project EdgeFLEX (grant no. 883710).

B. Literature Review

Several frequency estimation techniques have been proposed in the literature, categorized as analytical or signal processing approaches [2], [4]–[11]. Among these, we focus on the FDF, which is an analytical technique for estimating system bus frequencies using the rotor speeds of SMs [2]. Applications of the FDF are mostly in power system modeling [12], [13] and the state estimation [14], [15]. It should be noted that the FDF is a simulation tool and not a measurement to be implemented in online applications. However, the FDF can be inaccurate because it neglects the dynamics of any devices except for SMs. To overcome this issue, [16] developed a distributed FDF, considering the virtual inertia contributions of double-fed induction generators. This work further extends the FDF to include the dynamic effect of DER controllers. This is achieved by exploiting the concept of RoCoP proposed in [3].

Among the several control techniques of inverter-based resources [17]–[20], this paper studies DERs equipped with the two most prevalent controls, including droop-based grid-forming (GFM) and grid-following (GFL) controls, which are represented as current and voltage sources, respectively [17], [18]. Moreover, this paper investigates the effect of frequency control parameters, including the droop gain and the time constant of the low pass filter, on the frequency estimation.

C. Contributions

The contributions of the paper are as follows.

- The formulation of a generalization of the FDF in order to take into account the effect of the dynamics of the frequency controllers of DERs on the frequency estimation of system buses. Both grid-forming and grid-following schemes are considered. The proposed extended FDF has the same structure as the original formula presented in [2]. With this aim, the effect of DER controllers is defined in terms of equivalent virtual admittances and/or rotor speeds.
- The impact of the DERs' control settings on the system bus frequency estimation is addressed. This impact is assessed qualitatively in the case study.

D. Paper organization

The remainder of this paper is organized as follows. Section II recalls the derivation of the FDF based on the power flow equations and extends the formulation to take into account DERs' dynamics. Section III introduces a case study based on the IEEE 118-bus system to validate the proposed formula and then presents the results. Section IV concludes the paper.

II. Extended Frequency Divider Formula

This section briefly recalls the formulation of the frequency divider and its derivation based on the RoCoP. Subsection II-A reviews the FDF for buses where SMs are connected. Then, in Subsections II-B and II-C, the FDF is extended to show how frequency variations of buses connected to DERs spread across the whole power system. Finally, Subsection II-D presents the extended formulation of the FDF.

The foundation of the FDF in [3] is the power flow equations. This work shows that the power injections at network buses can be written as:

$$\boldsymbol{p}(t) = \boldsymbol{p}'(t) + \boldsymbol{p}''(t)\,, \tag{1}$$

where $\boldsymbol{p}'(t)$ is the quota of active power that contributes to frequency variations of buses, and $\boldsymbol{p}''(t)$ is the quota of active power that does not contribute to the frequency variations at the buses.

Assuming a steady-state model for the transmission lines, [3] shows that the rate of change of regulating active power injected at bus h, $\dot{p}'_h(t)$, is related to the variation of the bus frequencies as follows:

$$\dot{p}'_h(t) = -\Omega_b \sum_{k \in \mathbb{B}} B^{hk}_{\rm bus} \Delta\omega_{{\rm B},k}(t)\,, \tag{2}$$

where $\mathbb{B}$ is the set of the n system buses; $B^{hk}_{\rm bus}$ is the imaginary part of the element (h,k) of the system admittance matrix $\mathbf{Y}_{\rm bus} \in \mathbb{C}^{n\times n}$; $\Delta\omega_{{\rm B},k}$ is the frequency variation at bus k, and Ω_b is the synchronous speed in (rad/s). In vector form, (2) can be written as:

$$\dot{\boldsymbol{p}}'(t) = -\Omega_b \mathbf{B}_{\rm bus} \Delta\boldsymbol{\omega}_{\rm B}(t)\,, \tag{3}$$

Equation (3) is obtained considering only the network, i.e., independent of the type of device connected to bus h. To complete the analysis, one has thus to determine the expression of $\dot{p}'_h(t)$ for every device connected to the grid. Constant admittances show $\dot{p}'_h(t) = 0$ [3]. All other devices show $\dot{p}'_h(t) \neq 0$ and thus impact the frequency at their connection buses to the grid. Among those that impact the frequency to a greater extent, there are SMs and, as discussed in this work, DERs equipped with GFM or GFL controllers.

Subsection II-A reviews the case of SMs [3]. Then, Subsections II-B and II-C examine how the frequency control capability of DERs, including droop-based GFM and GFL, affect the ROCOP and, as a result, the frequency variations of all system buses.

A. Synchronous machine

The derivation of FDF based on voltage and current relationship in [2] gives:

$$\mathbf{B}_{\rm BG} \Delta\boldsymbol{\omega}_{\rm G}(t) = -(\mathbf{B}_{\rm bus} + \mathbf{B}_{\rm G}) \Delta\boldsymbol{\omega}_{\rm B}(t)\,, \tag{4}$$

where $\Delta\boldsymbol{\omega}_{\rm G}(t) \in \mathbb{R}^m$ is the vector of rotor speed variations of SMs, given by simulations; $\mathbf{B}_{\rm BG}$ is the imaginary part of $\mathbf{Y}_{\rm BG} \in \mathbb{C}^{n\times m}$, obtained from the extended admittance matrix, and $\mathbf{B}_{\rm G}$ is the imaginary part of $\mathbf{Y}_{\rm G} \in \mathbb{C}^{n\times n}$, a diagonal matrix whose h-th is either zero or the inverse of the SM reactance, depending on whether the machine is connected to bus h. The RoCoP injected at SMs' buses can be written by merging (3) and (4):

$$\dot{\boldsymbol{p}}'(t) = \Omega_b(\mathbf{B}_{\rm BG} \Delta\boldsymbol{\omega}_{\rm G}(t) - \mathbf{B}_{\rm G} \Delta\boldsymbol{\omega}_{\rm B}(t))\,, \tag{5}$$

or equivalently:

$$\dot{\boldsymbol{p}}'(t) = \Omega_b \mathbf{B}_{\rm BG}(\Delta\boldsymbol{\omega}_{\rm G}(t) - \Delta\boldsymbol{\omega}_{\rm BG}(t))\,, \tag{6}$$

where $\Delta\boldsymbol{\omega}_{BG}(t) \subset \Delta\boldsymbol{\omega}_{B}(t)$ is the vector of frequency variations at the buses adjacent to SM.

Equation (4) formulates the frequency divider for a grid that includes SMs and constant impedance loads exclusively. The expressions for DERs are not taken into account. The following subsections discuss DERs equipped with GFM and GFL control.

B. DER model with grid-forming control

Figure 1a models a DER as an ideal voltage source that is connected to bus h through a transformer or an inductor with reactance $b_{\rm M,h}$. Moreover, the DER is equipped with a GFM droop-based frequency control, as shown in Fig. 1c. The inner control loops and the reactive power control are neglected. It is demonstrated in [21] that a frequency droop control with a low pass filter, under specific conditions, is equivalent to a virtual synchronous machine (VSM). VSMs replicate the swing equation of SMs and provide virtual inertia to the power system.

Therefore, similar to SMs in (6), the RoCoP injected at DERs' buses with GFM control can be written as:

$$\Delta\dot{p}_h(t) = -\Omega_b b_{{\rm M},h}\big(\Delta\omega_{{\rm M},h}(t) - \Delta\omega_{{\rm B},h}(t)\big)\,, \tag{7}$$

where $b_{{\rm M},h}$ is assumed to be inductive and thus negative. In vector form, (7) becomes:

$$\dot{\boldsymbol{p}}'(t) = \Omega_b \mathbf{B}_{\rm BM}(\Delta\boldsymbol{\omega}_{\rm M}(t) - \Delta\boldsymbol{\omega}_{\rm BM}(t)) \tag{8}$$

where $\Delta\boldsymbol{\omega}_{\rm M}(t) \in \mathbb{R}^{d_m}$ is the vector of internal frequency variations imposed by DERs given by simulations; $\Delta\boldsymbol{\omega}_{\rm BM}(t) \subset \Delta\boldsymbol{\omega}_{B}(t)$ is the vector of frequency variations at the buses adjacent to DERs with GFM; $\mathbf{B}_{\rm BM}$ is the imaginary part of $\mathbf{Y}_{\rm BM} \in \mathbb{C}^{n\times d_m}$ obtained from the extended admittance matrix with DERs' connection reactances. Equations (3) and (8) formulate the frequency divider for a grid that includes DERs' buses exclusively with GFM controllers.

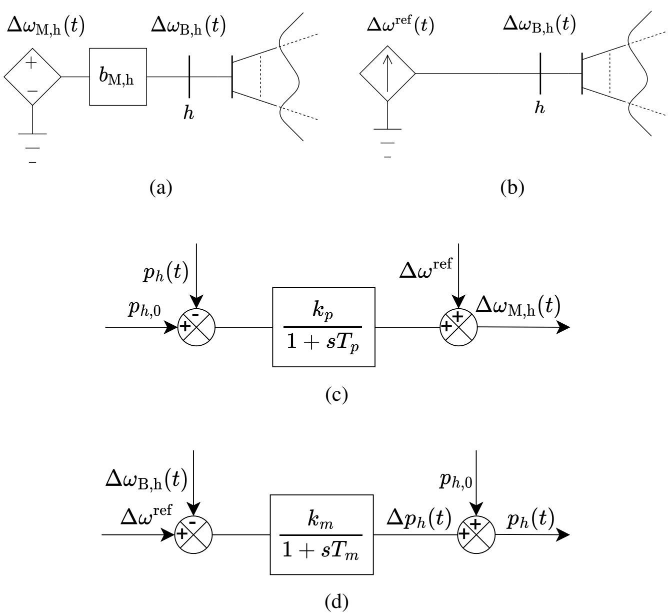

Fig. 1. (a) DER equivalent circuit as an ideal voltage source, (b) DER equivalent circuit as an ideal current source, (c) Grid-forming droop-based frequency control, (d) Grid-following droop-based frequency control.

C. DER model with grid-following control

Figure 1b shows a DER modeled as an ideal current source that is connected to bus h. Moreover, the DER is equipped with a GFL droop-based frequency control, as shown in Fig. 1d. The inner control loops and the reactive power control are neglected. The active power variation injected at bus h, $\Delta p_h(t)$, can be written as:

$$\Delta\dot{p}_h(t) = -\frac{\Delta p_h(t)}{T_m} + \frac{k_m}{T_m}\big(\Delta\omega^{\mathrm{ref}} - \Delta\omega_{\mathrm{B},h}(t)\big)\,, \tag{9}$$

where k_m is the GFL droop gain, T_m is the low pass filter time constant of GFL control, and $\Delta\omega^{\mathrm{ref}}$ is the variation of the reference frequency. Since, in general, the frequency reference does not change, one can assume $\Delta\omega^{\mathrm{ref}} = 0$. Then, (9) can be re-written as:

$$\Delta\dot{p}_h(t) = -\frac{\Delta p_h(t)}{T_m} - \frac{k_m}{T_m}\,\Delta\omega_{\mathrm{B},h}(t)\,. \tag{10}$$

It can be observed in a DER with a GFL control that the whole amount of the injected active power involves in modifying the bus frequency. One can thus assume that $\dot{p}_h(t) \approx \dot{p}'_h(t)$.[1]

Let us rewrite (10) as:

$$\dot{p}'_h(t) = \Omega_b\frac{k_m}{\Omega_b T_m}\big(\alpha_m\Delta p_h(t) - \Delta\omega_{\mathrm{B},h}(t)\big)\,, \tag{11}$$

where $\alpha_m = -(k_m)^{-1}$, or equivalently:

$$\dot{p}'_h(t) = \Omega_b B^h_{\mathrm{BL}}\big(\Delta\omega_{\mathrm{L},h}(t) - \Delta\omega_{\mathrm{B},h}(t)\big)\,, \tag{12}$$

[1]Reference [22] shows that, in effect, the term $\dot{p}''_h(t)$ is not always negligible. However, the approximation considered in this work introduces the same order of errors as the other simplifications (e.g., neglecting voltage magnitude variations) that lead to the definition of the FDF.

where $\Delta\omega_{\mathrm{L},h}(t) = \alpha_m\Delta p_h(t)$ can be considered as an equivalent internal frequency variation of the GFL control, which is a function of the control parameters and the active power variation of the DER; $B^h_{\mathrm{BL}} = k_m\,(\Omega_b T_m)^{-1}$ can be defined as an equivalent virtual admittance connecting the GFL converter at bus h to the grid. In vector form, (12) becomes:

$$\dot{\boldsymbol{p}}'(t) = \Omega_b\mathbf{B}_{\mathrm{BL}}\big(\Delta\boldsymbol{\omega}_{\mathrm{L}}(t) - \Delta\boldsymbol{\omega}_{\mathrm{BL}}(t)\big)\,, \tag{13}$$

where $\Delta\boldsymbol{\omega}_{\mathrm{BL}}(t) \subset \Delta\boldsymbol{\omega}_{\mathrm{B}}(t)$ is the vector of frequency variations at the buses adjacent to DERs with GFL.

D. Extended Frequency Divider Formula

The structure of the equations (6), (8), and (13) are similar and allows writing an extended version of the FDF, which formally has the same expression as the original FDF, but that is able to capture the dynamics of DERs with both GFM and GFL converters. First, let us define the vectors $\Delta\tilde{\boldsymbol{\omega}}_{\mathrm{G}} = (\Delta\boldsymbol{\omega}_{\mathrm{G}}, \Delta\boldsymbol{\omega}_{\mathrm{M}}, \Delta\boldsymbol{\omega}_{\mathrm{L}})$, and $\Delta\tilde{\boldsymbol{\omega}}_{\mathrm{BG}} = (\Delta\boldsymbol{\omega}_{\mathrm{BG}}, \Delta\boldsymbol{\omega}_{\mathrm{BM}}, \Delta\boldsymbol{\omega}_{\mathrm{BL}})$, and the matrix $\tilde{\mathbf{B}}_{\mathrm{BG}} = [\mathbf{B}_{\mathrm{BG}}, \mathbf{B}_{\mathrm{BM}}, \mathbf{B}_{\mathrm{BL}}]$, we obtain:

$$\dot{\boldsymbol{p}}'(t) = \Omega_b\tilde{\mathbf{B}}_{\mathrm{BG}}\big(\Delta\tilde{\boldsymbol{\omega}}_{\mathrm{G}}(t) - \Delta\tilde{\boldsymbol{\omega}}_{\mathrm{BG}}(t)\big)\,, \tag{14}$$

which can be rewritten in the same form as (4):

$$\tilde{\mathbf{B}}_{\mathrm{BG}}\Delta\tilde{\boldsymbol{\omega}}_{\mathrm{G}}(t) = -(\mathbf{B}_{\mathrm{bus}} + \tilde{\mathbf{B}}_{\mathrm{G}})\Delta\boldsymbol{\omega}_{\mathrm{B}}(t)\,, \tag{15}$$

where $\tilde{\mathbf{B}}_{\mathrm{G}}$ is the extended version of $\mathbf{B}_{\mathrm{G}}$ with the inclusion of the diagonal terms for the GFM and GFL converters. Equation (15) is the proposed extended formulation of the FDF.

III. Case study

In this section, the performance of the extended FDF is compared to the original FDF, given that DERs can regulate/impose frequency at their connection buses. The dynamics of DERs are represented by a droop control and a low pass filter in a grid-forming or a grid-following approach. The SMs are represented with a 4^{th}-order two-axis model and a speed governor. The simulation results are obtained using a modified IEEE 118-bus system built by substituting certain SMs with DERs of the same capacity. According to the penetration level of the non-synchronous generators, two cases are studied:

- Case 1: DERs account for 8.6% of the total generation, as shown in Fig. 2a.
- Case 2: DERs account for 76,1% of the total generation, as shown in Fig. 2b.

The disturbance is a 3-phase short-circuit fault at the line connecting buses 29 and 31, and near bus 31. The mentioned line is disconnected and reconnected when the fault is cleared after 0.15 s. The simulation time is 2 s, and the simulation time step is 0.01 s.

Figures 3 and 4 show the frequency variations of a load bus estimated with the FDF and the extended FDF, assuming that the DERs are equipped with GFM and GFL control, respectively. The difference between the frequency estimated with the FDF and the extended one becomes more noticeable in the high penetration case, both for GFM and GFL controls. This is because DERs have a greater contribution to the

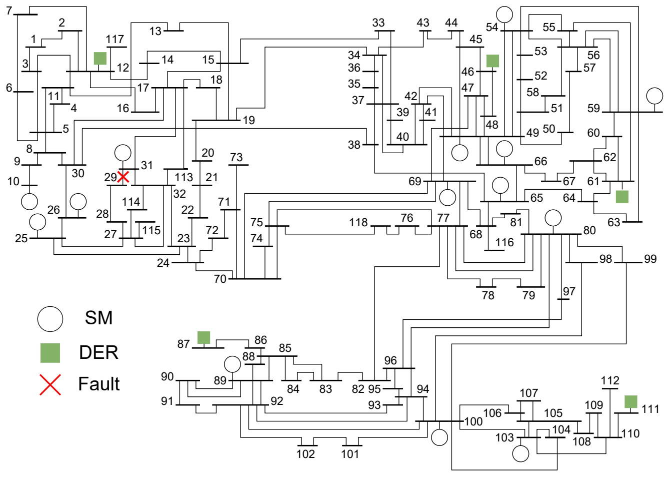

(a)

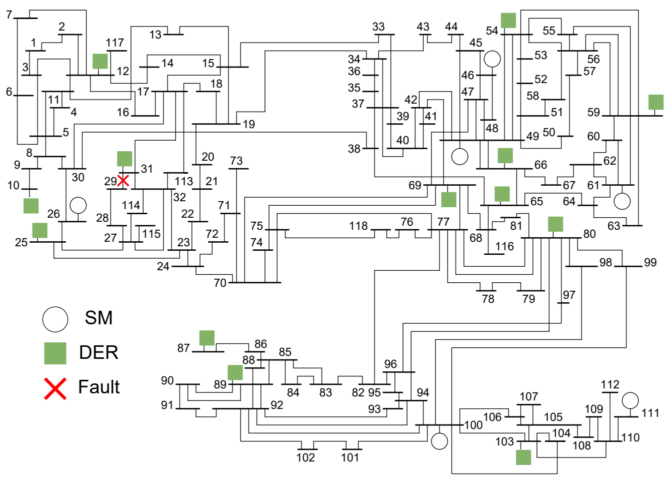

(b)

Fig. 2. Modified IEEE 118 test system. (a) case 1: Low penetration. DERs account for 8.6% of the generation, (b) case 2: High penetration. DERs account for 76.1% of the generation.

frequency control in a high penetration case, and the extended FDF captures this impact. Therefore, it is essential to take into account the dynamics of DERs in systems with high non-synchronous generator integration.

The effect of GFM control parameters on the frequency estimation is best shown in Fig. 5. The frequency estimated with the extended FDF is more damped than the FDF, and this damping is more evident with lower droop gains and higher time constants. This is because the RoCoP at the connection buses of the GFM converters is, respectively, directly and inversely proportional to the time constant and the droop gain.

Figure 6 shows the impact of the GFL control parameters on the frequency estimation. The frequency estimated using the extended FDF shows higher damping than the one estimated with the FDF. Moreover, RoCoP at the connection buses of GFL converters in (11) is, respectively, inversely and directly proportional to the time constant and the droop gain.

The difference between the frequency estimated by the

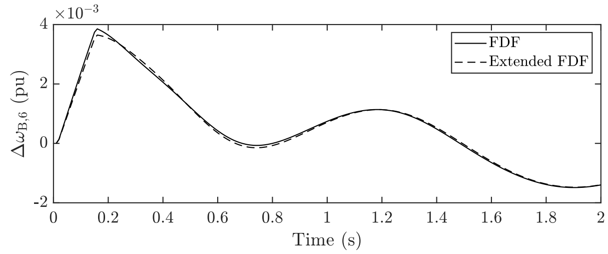

(a)

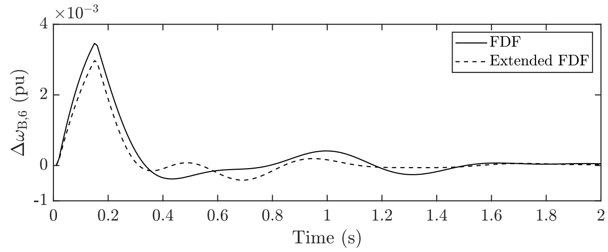

(b)

Fig. 3. Load bus frequency variation estimated with the FDF and the extended FDF for DERs with GFM control (k_p=0.02, T_p=0.2). (a) case 1: Low penetration, (b) case 2: High penetration.

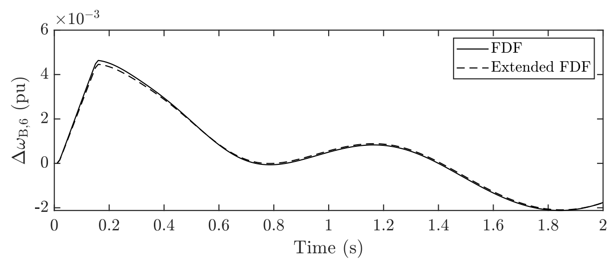

(a)

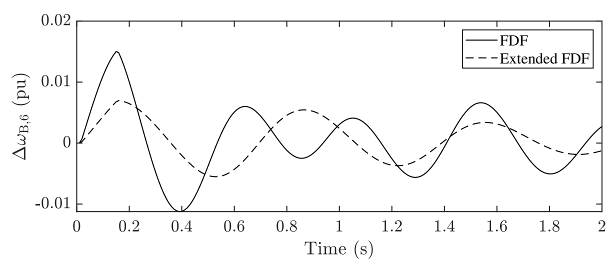

(b)

Fig. 4. Load bus frequency variation estimated with the FDF and the extended FDF for DERs with GFL control (k_m=50, T_m=0.4). (a) case 1: Low penetration, (b) case 2: High penetration.

extended FDF and the FDF is more evident as more DERs are integrated into the grid. In addition, when the control settings of the converters interfaced with the grid are taken into account, this difference becomes more distinct.

IV. Conclusions

This paper proposes an improvement to the frequency divider formula to estimate the local frequency variations of system buses more accurately, considering that DERs can control the frequency at their connection buses to the grid. Two frequency control techniques, including droop-based

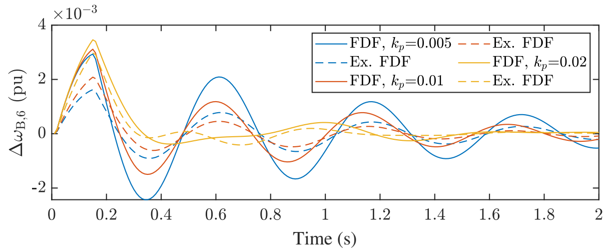

(a)

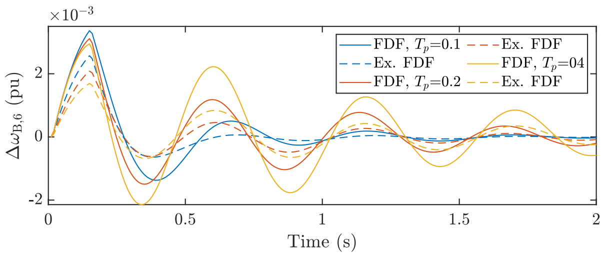

(b)

Fig. 5. Load bus frequency variation estimated with the FDF and the extended FDF for DERs with GFM control and (a) alternative droop gains, $T_p = 0.2$ (b) alternative time constants, $k_p = 0.01$.

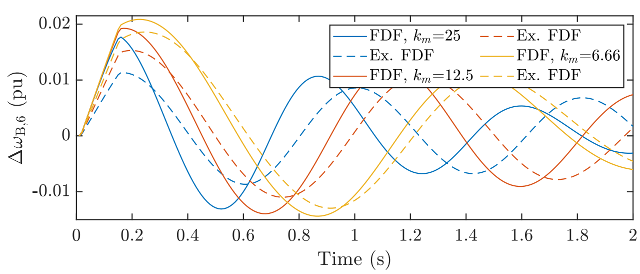

(a)

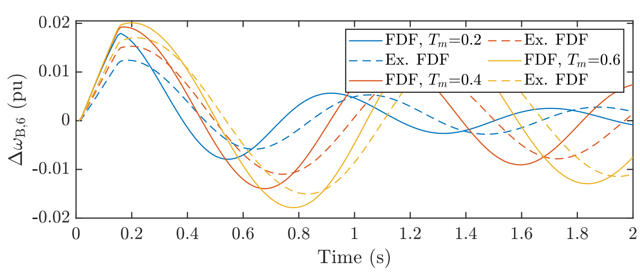

(b)

Fig. 6. Load bus frequency variation estimated with the FDF and the extended FDF for DERs with GFL control and (a) alternative droop gains, $T_m = 0.4$ (b) alternative time constants, $k_m = 12.5$.

GFM and GFL, are examined. The results show that: (i) for systems with significant penetration of non-synchronous sources, it is essential to consider the dynamics of DERs in the frequency divider formula; (ii) the estimated frequency using the proposed formula, which is an extended version of the frequency divider, dampens the oscillations; and (iii) the frequency estimation by the extended FDF is affected by the control settings of the DERs. Finally, the extended FDF can quantify whether the effect of DERs should considered or not. The original FDF can be used when differences are not significant. Future work will focus on the utilization of the proposed extended FDF to study the impact of DER control parameters on the overall frequency response of the grid and on the design of robust controllers able to take into account and properly exploit such an impact.

References

[1] F. Milano, F. Dörfler, G. Hug, D. J. Hill, and G. Verbič, "Foundations and challenges of low-inertia systems (invited paper)," in *2018 Power Systems Computation Conference (PSCC)*, 2018, pp. 1–25.

[2] F. Milano and Á. Ortega, "Frequency divider," *IEEE Trans. Power Syst.*, vol. 32, no. 2, pp. 1493–1501, 2016.

[3] F. Milano and A. Ortega, "A method for evaluating frequency regulation in an electrical grid–part i: Theory," *IEEE Trans. Power Syst.*, vol. 36, no. 1, pp. 183–193, 2020.

[4] J. Winkelman, J. Chow, B. Bowler, B. Avramovic, and P. Kokotovic, "An analysis of interarea dynamics of multi-machine systems," *IEEE Trans. Power Appar. Syst.*, no. 2, pp. 754–763, 1981.

[5] D. Fan and V. Centeno, "Phasor-based synchronized frequency measurement in power systems," *IEEE Trans. Power Deliv.*, vol. 22, no. 4, pp. 2010–2016, 2007.

[6] J. Nutaro and V. Protopopescu, "Calculating frequency at loads in simulations of electro-mechanical transients," *IEEE Trans Smart Grid*, vol. 3, no. 1, pp. 233–240, 2012.

[7] J. Zhao, Y. Tang, and V. Terzija, "Robust online estimation of power system center of inertia frequency," *IEEE Trans. Power Syst.*, vol. 34, no. 1, pp. 821–825, 2019.

[8] A. Bamigbade, V. Khadkikar, and M. Al Hosani, "Single-phase type-1 frequency-fixed fll for distorted voltage condition," *IEEE Trans. Ind. Electron.*, vol. 68, no. 5, pp. 3865–3875, 2020.

[9] F. Milano, "Complex frequency," *IEEE Trans. Power Syst.*, vol. 37, no. 2, pp. 1230–1240, 2022.

[10] S. Ghosh and M. E. Moursi, "An analytical approach for frequency estimation of modern power grid," *IEEE Trans. Power Syst.*, vol. 37, no. 5, pp. 4094–4097, 2022.

[11] H. Gao, H. Xin, L. Huang, Z. Li, W. Huang, C. Wu, and P. Ju, "Common-mode frequency in converter-integrated power systems: Definition, analysis, and quantitative evaluation," *IEEE Trans. Power Syst.*, vol. 37, no. 6, pp. 4846–4860, 2022.

[12] F. Milano, Á. Ortega, and A. J. Conejo, "Model-agnostic linear estimation of generator rotor speeds based on phasor measurement units," *IEEE Trans. Power Syst.*, vol. 33, no. 6, pp. 7258–7268, 2018.

[13] F. Arredondo, P. Ledesma, E. D. Castronuovo, and M. Aghahassani, "Stability improvement of a transmission grid with high share of renewable energy using tscopf and inertia emulation," *IEEE Trans. Power Syst.*, 2020.

[14] J. Zhao, L. Mili, and F. Milano, "Robust frequency divider for power system online monitoring and control," *IEEE Trans. Power Syst.*, vol. 33, no. 4, pp. 4414–4423, 2017.

[15] F. Milano, "Rotor speed-free estimation of the frequency of the center of inertia," *IEEE Trans. Power Syst.*, vol. 33, no. 1, pp. 1153–1155, 2017.

[16] B. Tan, J. Zhao, N. Duan, D. A. Maldonado, Y. Zhang, H. Zhang, and M. Anitescu, "Distributed frequency divider for power system bus frequency online estimation considering virtual inertia from dfigs," *IEEE J. Emerg. Sel. Top. Circuits Syst.*, vol. 12, no. 1, pp. 161–171.

[17] N. Pogaku, M. Prodanovic, and T. C. Green, "Modeling, analysis and testing of autonomous operation of an inverter-based microgrid," *IEEE Trans. Power Electron.*, vol. 22, no. 2, pp. 613–625, 2007.

[18] J. Rocabert, A. Luna, F. Blaabjerg, and P. Rodriguez, "Control of power converters in ac microgrids," *IEEE Trans. Power Electron.*, vol. 27, no. 11, pp. 4734–4749, 2012.

[19] X. Wang, M. G. Taul, H. Wu, Y. Liao, F. Blaabjerg, and L. Harnefors, "Grid-synchronization stability of converter-based resources—an overview," *IEEE Trans. Ind. Appl.*, vol. 1, pp. 115–134, 2020.

[20] R. Rosso, X. Wang, M. Liserre, X. Lu, and S. Engelken, "Grid-forming converters: Control approaches, grid-synchronization, and future trends – A review," *IEEE Trans. Ind. Appl.*, vol. 2, pp. 93–109, 2021.

[21] S. D'Arco and J. A. Suul, "Equivalence of virtual synchronous machines and frequency-droops for converter-based microgrids," *IEEE Trans Smart Grid*, vol. 5, no. 1, pp. 394–395, 2013.

[22] W. Zhong, G. Tzounas, and F. Milano, "Improving the power system dynamic response through a combined voltage-frequency control of distributed energy resources," *IEEE Trans. Power Syst.*, vol. 37, no. 6, pp. 4375–4384, 2022.